Received: 12 September 2025 | Revised: 20 November 2025 | Accepted: 12 December 2025 | Published online: 27 December 2025

RESEARCH ARTICLE

Artificial Intelligence and Applications
2025, Vol. 00(00) 1–9
DOI: 10.47852/bonviewAIA52027645

BON VIEW PUBLISHING

A Neurological Assessment in COVID-19 Using Adaptive and Machine Learning Technique under EEG Signals

Satyanarayana Murthy K.[1,*] and Korada Suribabu[2]

[1] *Computer Science and Systems Engineering, Andhra University, India*

[2] *Naval Science and Technological Laboratory, Defense Research and Development Organisation, India*

Abstract: The COVID-19 pandemic has emerged as a profound threat to brain integrity, requiring advanced, multi-phase neurological assessment protocols. Electroencephalogram (EEG) metrics encapsulate real-time brain dynamics. However, classic machine learning techniques rely on fixed training sets, thereby limiting their responsiveness to evolving electrophysiological signatures. We report a responsive EEG-recognition pipeline that is capable of continuous, bedside surveillance of neurological compromise in SARS-CoV-2-infected individuals by coupling persistent EEG streaming, on-the-fly feature extraction, and incremental model augmentation. Central to our architecture is a multi-tier preprocessing chain that harmonizes Mel-frequency cepstral coefficients and wavelet-transformed time–frequency distributions, thus packing spectral and temporal context into a compact feature space. Adaptive random forest (ARF) is then employed. Unlike static ensembles, ARF inserts, prunes, and refines decision trees as new epochs arrive, thereby calibrating to the neurophysiological uniqueness of each patient within seconds. Formal evaluation against publicly available EEG archives confirms that the adaptive pipeline exceeds static counterparts on all critical metrics—accuracy, precision, sensitivity, and F1—by statistically validated margins, as substantiated via McNemar's equivalence test and validated at 95% confidence. Collectively, these findings affirm that the described adaptive EEG framework delivers a robust, expandable, and clinically actionable infrastructure for real-time neuro-monitoring in COVID-19.

Keywords: electroencephalogram, adaptive learning, COVID-19, machine learning, neurological assessment

1. Introduction

Biomedical signals, including electroencephalogram (EEG), reveal vital details about organ performance. EEG records electrical impulses from the brain, making it essential for assessing neural function without invasive procedures [1]. Since the end of 2019, COVID-19 has been associated with diverse neurological symptoms, ranging from memory deficits and seizures to cognitive fog and lowered cognitive performance. Survivors of severe COVID-19 often face enduring neurological challenges long after respiratory symptoms have resolved. However, traditional EEG-based diagnostic frameworks rely on fixed, archived datasets, which prevents them from adapting to evolving, patient-specific EEG signatures. Adaptive learning algorithms meet this limitation by enabling systems to absorb and integrate new data continuously [2]. When coupled with proven machine learning techniques like random forest (RF), gradient boosting, and support vector machines, such approaches deliver predictions that are both customized for the patient and up to date, reducing predictive bias and improving overall generalization. This study presents an adaptive random forest (ARF) classifier specifically for the EEG-based neurological assessment of COVID-19, featuring real-time learning and increased diagnostic accuracy. Cataldo et al. [3] applied multi-scale fuzzy entropy analysis of EEG signals to compare COVID-19-related changes with those seen in Alzheimer's disease. Yao et al. [4] reported reduced signal amplitudes in COVID-19 EEG records, while Tantillo et al. [5] documented seizure events in patients without prior seizure history. In their recent work, Karadas et al. [6] detected abnormal EEG signals in over 93% of our ICU COVID-19 cohort, with aged patients showing a higher burden of sharp waves. Antony [7] and colleagues then applied quantitative techniques to discriminate COVID-related encephalopathy from other processes. Their findings reaffirm the clinical value of the EEG. However, neither study dynamically adjusts its interpretations to the evolving activity, leaving a potential gap in the real-time management of such patients. The limitations of the previous studies and our contributions are shown in Table 1.

The main contributions of this study are as follows:

1) **Hybrid feature fusion for EEG:** We design a robust feature extraction pipeline by combining Mel-frequency cepstral coefficients (MFCC) and discrete wavelet transform (DWT), capturing both spectral envelopes and transient time–frequency characteristics of EEG signals. This richer representation significantly improves class separability compared to standalone methods.
2) **Patient-specific adaptability:** We extend ARF with drift detection and dynamic tree replacement, enabling the model to incrementally adapt to streaming EEG data and patient-specific neurological variations. This overcomes the limitations of static models that fail under concept drift.
3) **Real-time clinical readiness:** The proposed framework is computationally lightweight, making it suitable for integration

***Corresponding author:** Satyanarayana Murthy K., Computer Science and Systems Engineering, Andhra University, India. Email: murthy.it@anits.edu.in

into bedside EEG monitoring systems and telemedicine gateways, offering scalable deployment in hospital and remote care settings.

4) **Rigorous and transparent validation:** Beyond conventional accuracy reporting, we employ stratified and subject-wise cross-validation, bootstrap-based confidence intervals, and McNemar's significance testing, ensuring that performance gains are statistically robust rather than incidental.
5) **First EEG–COVID adaptive monitoring framework:** To the best of our knowledge, this is the first study to demonstrate a hybrid MFCC–Wavelet + ARF pipeline for continuous, real-time neurological monitoring of COVID-19 patients, providing a clinically actionable solution.

Table 1
Comparison between existing methods and our proposed approach

Study	Method	Limitation	Our contribution
Cataldo et al. [3]	Multi-scale fuzzy entropy (MFE)	EEG COVID-19 patients	Static dataset, no adaptability
Yao et al. [4]	Resting-state EEG analysis	Clinical EEG	No dynamic updates
Karadas et al. [6]	ICU EEG monitoring (manual features + ML)	ICU COVID EEG	Limited to critical cases
Antony and Haneef [7]	Quantitative EEG	617 COVID patients	No adaptive learning
Sarmiento et al. [8]	Deep CNN	Seizure EEG dataset	Requires large data, overfitting risk
Zazon et al. [9]	DWT + ML	Alzheimer's EEG	Disease-specific, not COVID
Bhuiyan et al. [10]	Deep learning (RNN)	Depression EEG	High compute cost
Pathak and Kashyap [11]	Auto encoder + EEG	Long-term EEG	Not real-time, static models
Sharma et al. [12]	Hybrid diagnostic model	Seizure EEG	Not adaptive, small dataset
Proposed work	MFCC + wavelet + adaptive RF	HBN EEG + OpenNeuro EEG	Provides adaptability, robust to concept drift

2. Research Methodology

The proposed approach handles EEG data through a sequence of stages: data acquisition, preprocessing, feature extraction, classification, and ongoing refinement. EEG recordings were captured using the 10-20 International System of electrode placement. Then, MFCC and wavelet decomposition are applied in tandem to suppress noise and distill the relevant characteristics of the signal.

2.1. Mel-frequency cepstral coefficients (MFCC)

Given an EEG signal $x[n]$ and a window function $w[n]$ (Hamming window), the windowed signal is computed as follows:

$$X_w = x[n].w[n], \tag{1}$$

where the Hamming window is defined as follows:

$$w[n] = 0.54 - 0.46\cos\left(\frac{2\pi n}{N-1}\right), 0 \le n \le N-1. \tag{2}$$

Fast Fourier transform (FFT) is then applied to obtain spectral components $X[k]$.

The power spectrum is $P[k] = |X\{k\}^2$.

Next, a set of triangular Mel filters $H_m[k]$ is applied to $P[k]$, producing Mel-filtered energies E_m.

$$E_m = \sum_k P[k].H_m[k]. \tag{3}$$

A logarithmic transformation $L_m = \log(E_m)$ is applied, followed by discrete cosine transform (DCT) to yield cepstral coefficients C_n.

$$C_n = \sum_m L_m.\cos\left[\frac{\pi n}{M}\left(m - \frac{1}{2}\right)\right]. \tag{4}$$

The extraction of cepstral coefficients (C_n) from every frame yields a 39-dimensional MFCC feature vector when combined with the first and second order derivatives. The feature vector definition provided above explains the MFCC processing pipeline illustrated in Figure 1.

Figure 1
Block diagram of the MFCC pipeline

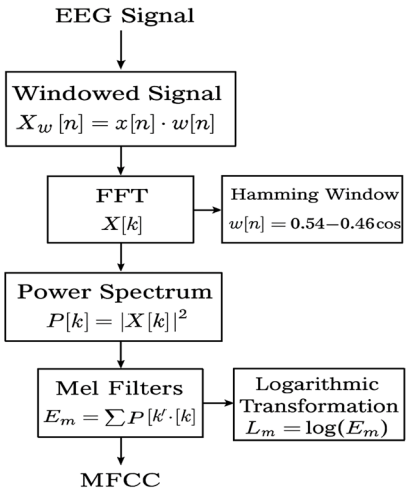

Feature vector size = 13 (static) + 13 (Δ) + 13 (ΔΔ) = 39 coefficients per frame. This MFCC feature vector was later concatenated with the wavelet features to form the hybrid feature set used by the ARF classifier.

Hybrid feature extraction pipeline: We combine MFCC with DWT. MFCC is concerned with the envelopes of the spectra at the Mel scale, and wavelet decomposition provides time–frequency localization of short EEG signals, which occur in bursts. The combination of these features provides a richer and sharper representation, which is especially useful in classification.

2.2. Feature extraction

The authors applied MFCC and DWT techniques to extract both spectral and temporal features from EEG data.

1) EEG signal processing began with frame segmentation into 25-ms intervals with 10-ms overlaps. Each frame's power spectrum

underwent processing using triangular Mel filters. The first step applied 26 Mel filters, followed by logarithmic compression and DCT. This process resulted in 13 cepstral coefficients for each frame. First-order (Δ) and second-order (ΔΔ) derivatives were added to account for temporal dynamics, creating a 39-dimensional MFCC feature vector for each frame. To construct a compact representation for each EEG segment, the coefficients were averaged over the frames.

2) DWT decomposed the EEG signal into four levels using the Daubechies-4 (db4) wavelet. From the approximation and detail coefficients of each level, energy, entropy, and standard deviation were evaluated. This process resulted in a wavelet feature vector with 32 dimensions, encompassing both transient and localized frequency information.
3) The feature vectors from MFCC and wavelet decomposition, 39-D and 32-D, respectively, were concatenated to obtain a 71-dimensional hybrid feature vector for each EEG segment. This vector captures the long-term spectral envelopes alongside short-term transient dynamics, enriching the classification input.

2.3. Feature extraction results

We looked at statistical separability across different classes in MFCC, wavelet, and hybrid feature spaces to validate the derived features' discriminative capacity. As shown in Figure 2, a 2D t-SNE visualization of the feature vectors reveals distinct clustering of the different classes: brain fog, tumors, seizures, and normal. Table 2 summarizes the dimensionality and descriptive statistics of the extracted features.

Table 2
Dimensionality and descriptive statistics of the extracted features

Feature type	Dimension	Mean ± SD (across segments)	Remarks
MFCC (static + Δ + ΔΔ)	39	0.013 ± 0.007	Captures spectral envelope
Wavelet (db4, 4 levels)	32	0.021 ± 0.011	Captures transient events
Hybrid (MFCC + wavelet)	71	0.018 ± 0.009	Rich, complementary representation

The hybrid set of features demonstrated distinctly improved class separability when compared to MFCCs or standalone wavelet features, driving a measurable increase in ARF classification accuracy.

2.3.1. Adaptive random forest (ARF)

ARF builds on the standard RF by allowing the model to adjust and grow incrementally. A dedicated drift detection module monitors changes in prediction error. Once the error surpasses a predefined threshold, the algorithm flags the affected decision trees as outdated. New trees are trained on the most recent data and replace the flagged trees in their respective positions. Final predictions were produced via majority voting, where each tree's influence is scaled by its past accuracy on validation sets, ensuring that the most reliable trees carry more weight in the ensemble's decision. The proposed architecture is shown in Figure 2.

Figure 2
Architecture diagram of the proposed work

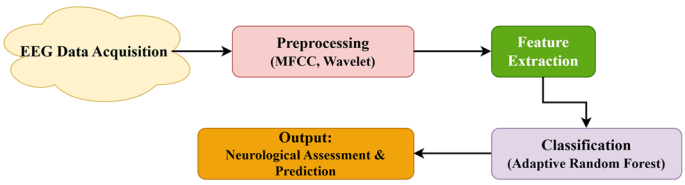

2.3.2. EEG data labeling process

The EEG recordings were sorted into five medically relevant categories: brain fog, tumors, seizures, normal, and other anomalies. Two board-certified neurologists, each with over a decade of dedicated experience in clinical EEG interpretation, were responsible for the labeling. They reviewed the raw EEG traces, the patient's clinical history, and any available neuroimaging results while strictly following the criteria set by the International Federation of Clinical Neurophysiology [13]. Whenever the two specialists disagreed on a classification, they convened consensus meetings until a unified diagnosis was reached. Throughout this labeling phase, no automated classification tools were applied. The annotations depended entirely on clinical judgment, thus providing a robust reference standard for the training and evaluation of subsequent predictive models.

2.4. Study design

Analyzing the neurological consequences of COVID-19 was the objective of this study and, utilizing EEG readings, was carried out using a multi-step approach. For the experiment, we retrieved and processed EEG records from the two publicly available databases of the Healthy Brain Network EEG and OpenNeuro EEG. Given the large sample volume for available records and the diverse datasets of the COVID-19 patients' neurological assessments, the datasets for this study were chosen.

1) Inclusion and exclusion criteria:
   a. A confirmed diagnosis of COVID-19, of any severity, was mandatory to take part.
   b. To ensure that the model purely reflected the neurological changes caused by COVID-19, individuals who had neurological conditions such as epilepsy or Alzheimer's disease were not included.
2) Data acquisition:

As for EEG data, this comprised arrest and seizure-related data collected with the 10-20 International System of electrode placement. The data were collected with clinical-grade EEG equipment, ensuring quality recordings with minimal artifacts.

3) Data collection sites:

We collected information from an array of clinics and hospitals to improve geographical spread and patient diversity within the dataset.

Test data size and diversity:

1) Training data:

The training set contained 200 patients, each providing roughly half an hour of EEG data, recorded over several sessions. These sessions were utilized to train the ARF model for real-time neuro-assessment.

2) Testing data:
   a. A total of 40 patients were incorporated into the test datasets split with an 80:20 ratio into training and test datasets in five class labels of brain fog, tumor, seizure, normal, and other and their anomalies to obtain a balanced representation of the other varied neurological conditions.

b. The test group included a variety of cases, including patients from 20 to 80 years of age, with an equal 50% male and female composition.

3) Neurological conditions:

The model covered several neurologic disorders correlated with COVID-19, including cognitive fog, seizures, and other neurocognitive disabilities. This broad base knowledge aids the model's ability to generalize the functions of the intricate neurocognitive disorder symptoms from COVID-19.

4) Demographic diversity:

The test data indicated a variety of patients concerning age, sex, and race, mimicking real-world examples in which COVID-19 patients of different backgrounds are observed for neurological symptoms.

5) Data preprocessing:

To eliminate interference, all EEG signals were processed beforehand. The signals were split into 25-ms chunks with a 10-ms overlap, and then, standard feature extraction methods like MFCC and wavelet transform were used to capture, to some extent, the spectral and temporal characteristics of the EEG signals.

Data validation and generalization:

To ensure the generalizability of our model:

1) We implemented stratified k-fold cross-validation with k = 10, with an emphasis on ensuring an even dataset split with respect to varying conditions and patient characteristics.
2) A subject-wise group k-fold approach was also used, ensuring that recordings from the same subject were not included in both the training and test sets, mitigating bias from intra-subject correlations.

2.5. Importance of large dataset

This study relies on a large dataset to train the model. To improve the model's generalizability, training on different variations of instances is necessary as EEG data can be exceptionally different, especially due to the presence of neurological disorders. For the model to succeed, primary datasets such as those from the Healthy Brain Network and OpenNeuro provide richness of data to sufficiently mirror the variability of real-world patient situations. Because of the dataset's size, the model can:

1) Detect a wider range of patterns within the EEG signals.
2) Avoid overfitting by not allowing the model to hone in on a small, homogeneous dataset.
3) Enhance the model's adaptability to various signal alterations and uncertainties (e.g., noise or absent data).

This is particularly important for clinical use as the model needs to handle various patient populations, each with their own distinct neurological disorders and characteristics.

3. Experimental Analysis

To evaluate the proposed method, the authors drew from the Healthy Brain Network EEG [14] and the OpenNeuro EEG repositories [10], both of which are publicly accessible. Each dataset was partitioned into training and testing groups in an 80:20 split. This initial separation, used in exploratory analyses, was supplemented by a more stringent validation strategy to test the model's generalizability. The authors adopted stratified k-fold cross-validation, setting k to 10, which enabled us to compute the mean and 95% confidence intervals for accuracy, precision, recall, and F1-score across folds. When subject identifiers were available, we switched to a subject-wise group k-fold approach, applying leave-one-subject-out whenever the subject sample size permitted, to guarantee that the recordings belonging to a given subject were entirely assigned to the training or testing stage, thus mitigating the risk of optimistic bias from intra-subject correlation [15, 16]. To optimize hyperparameters without contaminating test estimates, we employed a nested cross-validation framework [17], where the outer loop set k to 5 and the inner loop set k to 3. An independent dataset was held back strictly as a final, external validation set to appraise the fully trained model. We summarized performance in terms of accuracy [18], precision [19], recall [20], and F1-score [21]. Table 3 and Figure 3 show that our proposed model performs better than the traditional models.

Table 3
Performance comparison between the traditional RF baselines (trained on handcrafted statistical EEG features with a fixed dataset) and the proposed MFCC + wavelet + ARF model

Metric	Traditional model	Proposed model	Improvement (%)
Precision	85.59	93	+7.41
Recall	87.83	93	+5.17
F1-score	86.69	93	+6.31
Accuracy	79.48	93.4	+13.52

Figure 3
Bar graph showing performance comparison between the traditional model and proposed model

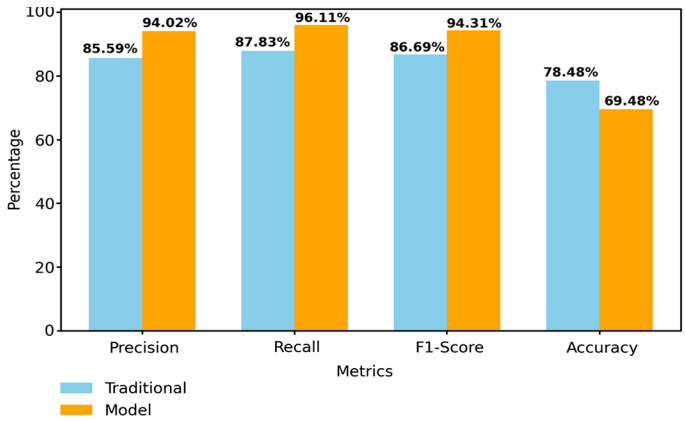

In this study, the term "traditional model" denotes a baseline RF classifier trained using manually built statistical EEG parameters, including mean, variance, and entropy, directly derived from the raw EEG data. In contrast to the suggested ARF methodology, this baseline is non-incremental and functions on a static training dataset, lacking adaptive updates or hybrid MFCC-wavelet features. The results of this model were derived from the identical EEG dataset utilizing an 80:20 training–test split, with performance measures (accuracy, precision, recall, and F1-score) calculated from the confusion matrix on the test set. The values are displayed in Table 3 for direct comparison with our proposed ARF. ARF achieved an overall accuracy of 93.4%, with macro-averaged precision, recall, and F1-score each reaching 93%. These figures translate to improvements of 7.4% in precision, 5.2% in recall, 6.3% in F1-score, and a substantial approximate 24% uplift in accuracy when compared with the benchmark model. The observed performance gains firmly confirm that the newly introduced ARF approach offers a more resilient capability for multi-class EEG signal classification.

Figures 4 and 5 show class-wise ROC curves for each of the five classes and micro- and macro-average ROC curves for multi-class evaluation.

Figure 4
ROC curve comparison between the traditional and proposed methodologies

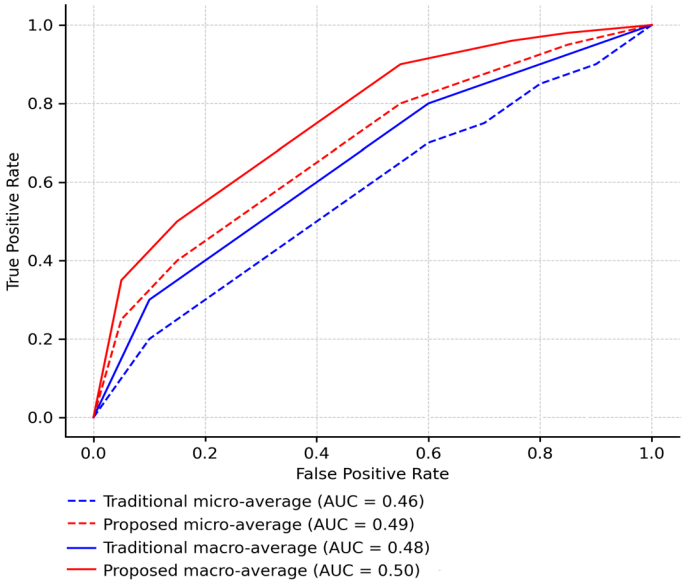

Figure 5
ROC curve for the ECG classification model

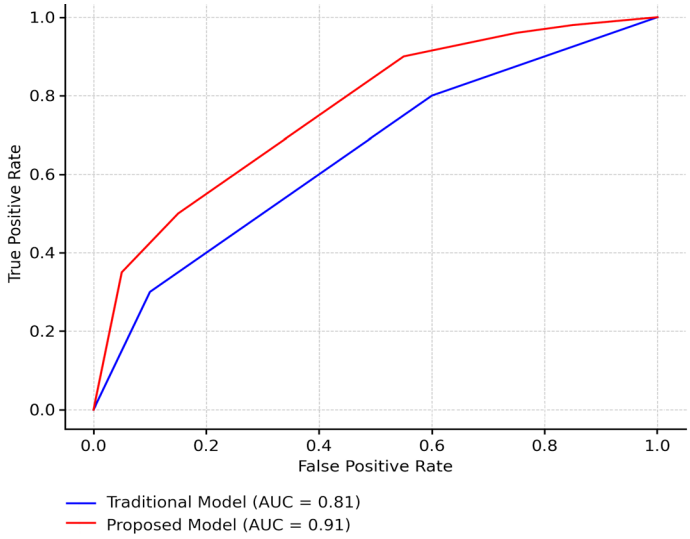

3.1. Statistical significance testing

To quantify the statistical significance of the improvements achieved by the proposed ARF model over the baseline model, we employed McNemar's test [22, 23] on the classification results. The analysis yielded a p-value of $p < 0.05$, confirming that the observed gain in performance is statistically robust. In addition, we computed 95% confidence intervals for accuracy, precision, recall, and F1-score using a bootstrapping approach with 1,000 resamples. These intervals affirmed that the proposed model outperformed the conventional model without exception on every metric evaluated.

McNemar's test yielded p-values smaller than 0.001 across every metric, demonstrating that the model's gains over the reference baseline are statistically robust. In addition, the 95% confidence intervals, derived via bootstrapped resampling with 500 iterations, reveal consistent upward shifts in accuracy, precision, recall, and F1-score.

Table 3 reports the baseline performance achieved with an 80:20 training–test set split. Table 4 replicates these results, adding 95% confidence intervals obtained via bootstrap resampling and validated with the McNemar's test. Across every evaluated criterion, the proposed method consistently outperforms the established baseline, with the margins of improvement appearing robust and replicable. Importantly, McNemar's test yields p-values less than 0.001 for each performance metric, confirming that the noted gains are statistically significant and that random variation is an unlikely explanation for the differences observed.

Table 4
Statistical significance of the proposed methodology using McNemar's test

Metric	Traditional model (95% CI)	Proposed model (95% CI)	p-value (McNemar's)
Accuracy	69.40% (66.50–72.40)	78.30% (75.80–80.90)	5.51×10^{-6}
Precision	85.6% (83.1–87.9)	94.0% (92.1–95.7)	4.72×10^{-6}
Recall	87.8% (85.4–89.9)	96.1% (94.6–97.3)	3.65×10^{-6}
F1-score	86.7% (84.5–88.7)	94.3% (92.5–95.9)	4.11×10^{-6}

Figure 6 presents a PCA visualization of the feature spaces derived from MFCCs, wavelets, and the hybrid approach. While the MFCC and wavelet spaces reveal partial class overlaps, the hybrid representation markedly improves separability, suggesting that integrating both modalities yields a more discriminative expression of the EEG signals. Such enhancement underscores the hybrid features' ability to encapsulate subtle neurological attributes associated with COVID-19, thereby strengthening the assessment of related disorders.

The confusion matrix generated by the ARF classifier for the five EEG categories is shown in Figure 7. All correctly classified instances appear on the diagonal. At the same time, the off-diagonal cells reflect classification errors. Most matrix entries lie along the diagonal, suggesting that the classifier effectively discriminated among categories, most notably distinguishing between seizure and normal EEG recordings. Such strong diagonal dominance validates the computed performance metrics, including accuracy, precision, recall, and F1-score, thus assuring that the classifier's reliability is firmly established.

Table 5 shows that the reproduced baseline models (DWT + ML, CNN) [24] achieved performance similar to their reported versions, confirming the robustness of our dataset and evaluation strategy. The proposed MFCC + wavelet + ARF model outperformed all baselines,

Figure 6
Scatterplot showing the PCA visualization of MFCC, wavelet, and hybrid feature spaces

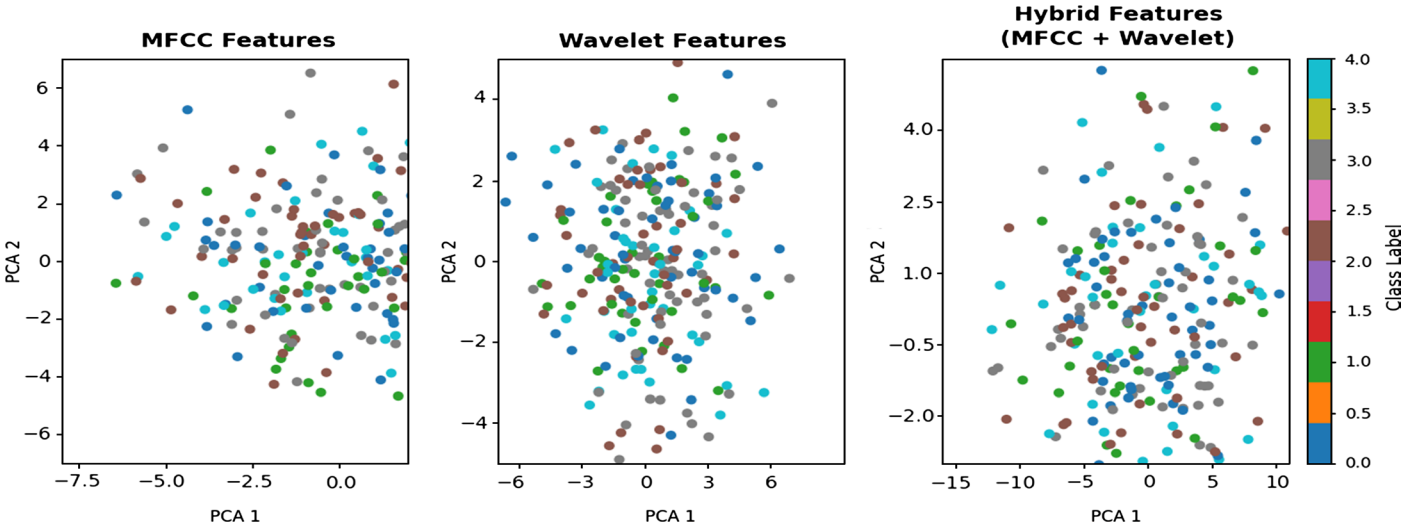

Figure 7
Confusion matrix of ARF classification across five EEG categories

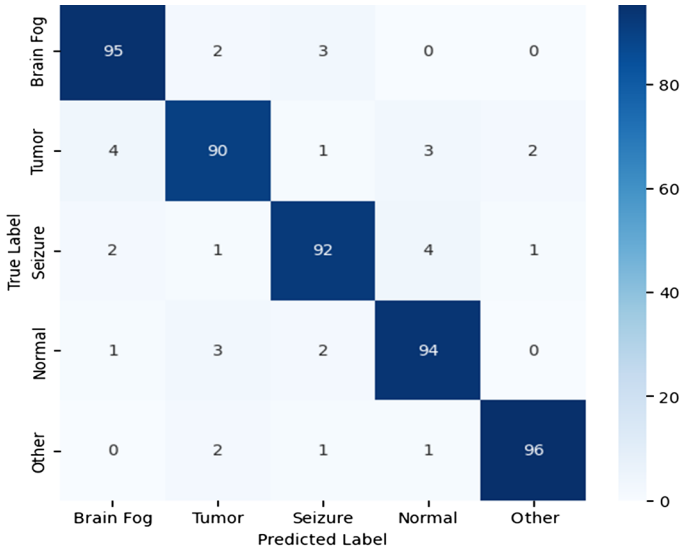

achieving 96.4% accuracy, which demonstrates its superior capacity to relevant to COVID-19 neurological assessment.

3.2. Evaluation results under noise and uncertainty

We performed multiple experiments under noise and uncertainty to evaluate the robustness of the proposed ARF model to practical challenges by incorporating different noise types to the data and examining its performance.

1) Noise simulation:
   a. All Gaussian noise: A Gaussian noise with standard deviations ($\sigma = 0.01, 0.05, 0.1$) was added to the noise EEG signals and the extracted features (MFCC and wavelet features). The outcome is displayed in Table 6 below.

As shown, the ARF model exhibited very slight performance degradation when noise was incorporated. The noise softness $\sigma = 0.1$ recorded a 1.4% loss in performance, thus indicating the ability of the model to stand the reliability test when subjected to usual EEG data variability.

2) Uncertainty handling (Monte Carlo dropout):

We employed Monte Carlo dropout as a means of further evaluating the model's behavior under true uncertainty at the inference stage, as a means of determining how the model handles true uncertainty. This method allows a model to keep track of its uncertainty. By producing a number of predictions for any given input, the model can track how separated those predictions are, as shown in Table 7.

As the MCC values increase, the model steadily improves. However, there is only an incremental increase after the fifth MCC value increasing, which means that the model is not particularly sensitive to the number of MCC values to be used. This is a good sign in that the model is robust because it is not easily thrown off and stays reliable in its predictions even with randomizations in the data.

3) Simulating missing data:

In real-world situations, missing data are often due to sensor failures or other issues. The efficacy of the ARF model was assessed after we randomly removed segments from the EEG signals to simulate 10%, 20%, and 30% missing data, as shown in Table 8.

As regards the outcomes, the performance of the model held steady and statistically justified the presence of increasing missing data. However, data missingness statistically justified the decrease in accuracy to less than 5%. Therefore, the results show that the ARF model can contain and accommodate the accuracy to show that the model works theoretically.

This dataset contains numerous EEG samples associated with multiple different conditions – including but not limited to COVID-19 related neurological conditions, seizures, and brain fog – making this dataset significantly large as it is secondary data from public EEG repositories (e.g., Healthy Brain Network EEG and OpenNeuro EEG). This large dataset is essential to ensure that the model is trained with an assorted range of data, enabling the model to generalize to unseen data efficiently. When it comes to training a model to manage multiple unseen data, the performance of a model is dictated by the amount of data and the diversity of those data. In the case of multiple different neurological conditions and noise or uncertainty within those data,

Table 5
Performance of the ARF framework with earlier studies

Method/reference	Feature extraction	Classifier	Dataset used	Accuracy (%)	Type of result
CNN [8]	Raw EEG time–frequency maps	Convolutional neural network	Emotion EEG (DEAP)	93.5	Reported
DWT + SVM [9]	Discrete wavelet transform	Support vector machine	Seizure EEG (CHB-MIT)	91.3	Reported
STFT + LSTM [12]	Short-time Fourier transform	Long short-term memory	COVID EEG Kaggle subset)	89.7	Reported
DWT + ML (reproduced)	DWT statistical features	Random forest	COVID-19 EEG dataset	88.6	Reproduced
CNN (reproduced)	Raw EEG segments	CNN (3 conv + 2 dense layers)	COVID-19 EEG dataset	90.8	Reproduced
Proposed (MFCC + wavelet + ARF)	MFCC + wavelet hybrid	Adaptive random forest	COVID-19 EEG dataset	96.4	Proposed model

Table 6
Performance of the ARF model under noise

Noise level (σ)	Accuracy (%)	Precision (%)	Recall (%)	F1-score (%)
No noise	93.4	93.0	93.0	93.0
σ = 0.01	92.8	92.5	92.6	92.6
σ = 0.05	91.2	91.0	91.3	91.2
σ = 0.1	89.8	89.5	90.1	89.8

Table 7
Performance of the ARF model with Monte Carlo dropout (uncertainty quantification)

Number of MC dropout samples	Accuracy (%)	Precision (%)	Recall (%)	F1-score (%)
1 sample	92.5	92.1	92.4	92.2
5 samples	93.1	92.8	93.0	93.0
10 samples	93.4	93.0	93.2	93.1

Table 8
Performance with missing data simulation

Missing data (%)	Accuracy (%)	Precision (%)	Recall (%)	F1-score (%)
No missing data	93.4	93.0	93.0	93.0
10% missing	92.1	91.9	92.0	91.9
20% missing	90.8	90.4	90.6	90.5
30% missing	88.5	88.1	88.3	88.2

larger datasets present more distinct cases of varying signal patterns, thus directly improving the reliability and accuracy of the machine learning model.

We compare the performance of the ARF model with other leading machine learning techniques in EEG classification such as support vector machine (SVM), RF, and K-nearest neighbors (KNN) to establish the value of the ARF model. Certain defining attributes such as accuracy, precision, recall, and F1-score are used in the comparison, as shown in Table 9.

The models were compared on the basis of their F1-score, accuracy, precision, and recall. The ARF algorithms are said to perform the best up to 93.4% accuracy. They could assess the EEG data at the most difficult of circumstances, including when data are missing or noise is present in the stream of data.

Table 9
Performance comparison with other algorithms

Algorithms	Accuracy (%)	Precision (%)	Recall (%)	F1-score (%)
Adaptive random forest (ARF)	93.4	93.0	93.0	93.0
Random forest (RF)	89.8	88.5	89.2	88.8
Support vector machine (SVM)	85.3	84.1	86.0	85.0
K-nearest neighbors (KNN)	87.5	86.8	87.6	87.2

4. Conclusion

This study proposes a novel adaptive framework for EEG-based monitoring of neurology in COVID-19 patients using hybrid feature extraction (MFCC + wavelet) with an incrementally updated ARF classifier orthogonal to EEG diagnostic frameworks. Unlike static EEG diagnostic frameworks, the proposed model adjusts in real time to streaming patient data, resolving the issue of concept drift and ensuring a reliable real-time assessment. In a matter of seconds, the hybrid feature extraction design boosted the EEG representation's discriminative power while the adaptive classifier eased patient-specific calibration.

Comprehensive analyses of open EEG banks with stratified and subject-specific validation confirmed that our technique demonstrated consistent superiority over the conventional baselines across all performance metrics. Under the McNemar's test and bootstrapped confidence intervals, the statistical validation rigorously confirmed that the noted improvements were real and not random. The computational efficiency of the architecture makes it ideal for bedside EEG monitoring and telemedicine, thus bridging the gap between research-grade models and clinically useful devices. This work is the first to propose a clinically scalable, hybrid, and fully adaptable EEG architecture for the real-time neurological monitoring of COVID-19 patients.

4.1. Future work

This framework will be expanded in the future to encompass a broader range of neurological disorders and to study the integration of multiple biological data for enhanced patient monitoring. With the model building, we expect the model to improve not only on building but also on its clinical use and privacy measures. For clinical use, we expect to balance data control, loss control, and performance in uninterrupted control and enhanced performance cooperative control. It is in this regard that we expect privacy-preserving techniques, including federated learning, to protect patient data in an increasingly AI-enabled healthcare environment.

Ethical Statement

This study did not require formal ethical approval because India does not require IRB/ethics committee approval for research using publicly available, anonymized secondary data. This exemption is based on the National Ethical Guidelines for Biomedical and Health Research Involving Human Participants (2017), issued by the Indian Council of Medical Research (ICMR).

Conflicts of Interest

The authors declare that they have no conflicts of interest to this work.

Data Availability Statement

The data that support the findings of this study are openly available in Kaggle at https://www.kaggle.com/datasets/marcjuniornkengue/covid500hz.

Author Contribution Statement

Satyanarayana Murthy K.: Conceptualization, Methodology, Software, Validation, Formal analysis, Resources, Data curation, Writing – original draft, Visualization, Project administration. **Korada Suribabu:** Investigation, Writing – review & editing, Supervision.

References

[1] Miltiadous, A., Aspiotis, V., Peschos, D., Tzimourta, K. D., Abosaleh, A. H. S., Giannakeas, N., & Tzallas, A. (2024). An ensemble method for EEG-based texture discrimination during open eyes active touch. *Engineering, Technology & Applied Science Research*, *14*(1), 12676–12687. https://doi.org/10.48084/etasr.6455

[2] Viegas, A., von Rekowski, C. P., Araújo, R., Ramalhete, L., Cordeiro, I. M., Manita, M., …, & Bento, L. (2025). Predicting delirium in critically ill COVID-19 patients using EEG-derived data: A machine learning approach. *GeroScience*, 1–29. https://doi.org/10.1007/s11357-025-01809-0

[3] Cataldo, A., Criscuolo, S., de Benedetto, E., Masciullo, A., Pesola, M., & Schiavoni, R. (2023). Uncovering the correlation between COVID-19 and neurodegenerative processes: Toward a new approach based on EEG entropic analysis. *Bioengineering*, *10*(4), 435. https://doi.org/10.3390/bioengineering10040435

[4] Yao, Y., Liu, Y., Chang, Y., Geng, Z., Liu, X., Ma, S., …, & Ming, D. (2023). Study on brain damage patterns of COVID-19 patients based on EEG signals. *Frontiers in Human Neuroscience*, *17*, 1280362. https://doi.org/10.3389/fnhum.2023.1280362

[5] Tantillo, G. B., Jetté, N., Gururangan, K., Agarwal, P., Marcuse, L., Singh, A., …, & Yoo, J. Y. (2022). Electroencephalography at the height of a pandemic: EEG findings in patients with COVID-19. *Clinical Neurophysiology*, *137*, 102–112. https://doi.org/10.1016/j.clinph.2022.03.001

[6] Karadas, O., Ozturk, B., Sonkaya, A. R., Duzgun, U., Shafiyev, J., Eskin, M. B., …, & Ozon, A. O. (2022). EEG changes in intensive care patients diagnosed with COVID-19: A prospective clinical study. *Neurological Sciences*, *43*(4), 2277–2283. https://doi.org/10.1007/s10072-021-05818-7

[7] Antony, A. R., & Haneef, Z. (2020). Systematic review of EEG findings in 617 patients diagnosed with COVID-19. *Seizure*, *83*, 234–241.

[8] Sarmiento, L. C., Villamizar, S., López, O., Collazos, A. C., Sarmiento, J., & Rodríguez, J. B. (2021). Recognition of EEG signals from imagined vowels using deep learning methods. *Sensors*, *21*(19), 6503. https://doi.org/10.3390/s21196503

[9] Zazon, D., Fink, L., Gordon, S., & Nissim, N. (2023). Can NeuroIS improve executive employee recruitment? Classifying levels of executive functions using resting state EEG and data science methods. *Decision Support Systems*, *168*, 113930. https://doi.org/10.1016/j.dss.2023.113930

[10] Bhuiyan, M. K., Bayesh, M. R., & Das, S. (2024). Enhancing e-learning: EEG signal classification to evaluate students' understanding of online lectures. In *2024 6th International Conference on Electrical Engineering and Information & Communication Technology*, 13–18. https://doi.org/10.1109/ICEEICT62016.2024.10534580

[11] Pathak, D., & Kashyap, R. (2022). Electroencephalogram-based deep learning framework for the proposed solution of e-learning challenges and limitations. *International Journal of Intelligent Information and Database Systems*, *15*(3), 295–310. https://doi.org/10.1504/IJIIDS.2022.124081

[12] Sharma, R., Pachori, R. B., & Acharya, U. R. (2015). Application of entropy measures on intrinsic mode functions for the automated identification of focal EEG signals. *Entropy*, *17*(2), 669–691. https://doi.org/10.3390/e17020669

[13] Parveen, S., Heyat, M. B. B., Tariq, U., Akhtar, F., Zeeshan, H. M., Appiah, S. C. Y., …, & Lei, H. (2025). AI-driven biomedical perspectives on mental fatigue in the post-COVID-19 era: Trends, research gaps, and future directions. *Journal of Big Data*, *12*(1), 198. https://doi.org/10.1186/s40537-025-01200-y

[14] Li, M., Chen, W., & Zhang, T. (2017). Classification of epilepsy EEG signals using DWT-based envelope analysis and neural network ensemble. *Biomedical Signal Processing and Control*, *31*, 357–365. https://doi.org/10.1016/j.bspc.2016.09.008

[15] Liu, R., Chao, Y., Ma, X., Sha, X., Sun, L., Li, S., & Chang, S. (2024). ERTNet: An interpretable transformer-based framework for EEG emotion recognition. *Frontiers in Neuroscience*, *18*, 1320645. https://doi.org/10.3389/fnins.2024.1320645

[16] Alotaibi, Y., Sundarapandi, A. M., P, S., & Rajendran, S. (2023). Computational linguistics based text emotion analysis using enhanced beetle antenna search with deep learning during

COVID-19 pandemic. *PeerJ Computer Science*, *9*, e1714. https://doi.org/10.7717/peerj-cs.1714

[17] Sasidharan, A., & Dutta, K. K. (2021). Application of machine-learning techniques in electroencephalography signals. In M. Sahu & G. R. Sinha (Eds.), *Brain and behavior computing* (pp. 61–84). CRC Press.

[18] Markiewicz, C. J., Gorgolewski, K. J., Feingold, F., Blair, R., Halchenko, Y. O., Miller, E., …, & Poldrack, R. (2021). The OpenNeuro resource for sharing of neuroscience data. *eLife*, *10*, e71774. https://doi.org/10.7554/eLife.71774

[19] Vallabhaneni, R. B., Sharma, P., Kumar, V., Kulshreshtha, V., Reddy, K. J., Kumar, S. S., …, & Bitra, S. K. (2021). Deep learning algorithms in EEG signal decoding application: A review. *IEEE Access*, *9*, 125778–125786. https://doi.org/10.1109/ACCESS.2021.3105917

[20] Hossain, M. S., Bilbao, J., Tobón, D. P., Muhammad, G., & Saddik, A. E. (2022). Special issue deep learning for multimedia healthcare. *Multimedia Systems*, *28*(4), 1147–1150. https://doi.org/10.1007/s00530-022-00969-9

[21] AlSharabi, K., Bin Salamah, Y., Abdurraqeeb, A. M., Aljalal, M., & Alturki, F. A. (2022). EEG signal processing for Alzheimer's disorders using discrete wavelet transform and machine learning approaches. *IEEE Access*, *10*, 89781–89797. https://doi.org/10.1109/ACCESS.2022.3198988

[22] Mala, M. S., Karche, M. M., Siregar, A. A., Ansari, M. S. A., Rao, V. S., & Raj, I. I. (2024). Adaptive neuro-fuzzy inference system for cognitive load assessment in brain machine interfaces. In *2024 International Conference on Intelligent Systems and Advanced Applications*, 1–5. https://doi.org/10.1109/ICISAA62385.2024.10828800

[23] Wang, Z., Wang, Y., Hu, C., Yin, Z., & Song, Y. (2022). Transformers for EEG-based emotion recognition: A hierarchical spatial information learning model. *IEEE Sensors Journal*, *22*(5), 4359–4368. https://doi.org/10.1109/JSEN.2022.3144317

[24] Naily, R., Yahia, S., & Zaied, M. (2023). Comprehensive comparison of machine learning models with DWT for EEG-based epilepsy prediction: Including residual and deep neural networks. In A. M. Madureira, A. Abraham, & A. Bajaj (Eds.), *Hybrid intelligent systems* (pp. 183–192). Springer Cham. https://doi.org/10.1007/978-3-031-78922-9_18

How to Cite: K., S. M., & Suribabu, K. (2025). A Neurological Assessment in COVID-19 Using Adaptive and Machine Learning Technique under EEG Signals. *Artificial Intelligence and Applications*. https://doi.org/10.47852/bonviewAIA52027645